Investigating the significance of zero-point motion in small molecular clusters of sulphuric acid and water

Jake L. Stinson,[1,a)] Shawn M. Kathmann,[2] and Ian J. Ford[1]
[1]*Department of Physics and Astronomy and London Centre for Nanotechnology, University College London, Gower Street, London WC1E 6BT, United Kingdom*
[2]*Physical Sciences Division, Pacific Northwest National Laboratory, Richland, Washington 99352, USA*

(Received 10 June 2013; accepted 19 December 2013; published online 10 January 2014)

The nucleation of particles from trace gases in the atmosphere is an important source of cloud condensation nuclei, and these are vital for the formation of clouds in view of the high supersaturations required for homogeneous water droplet nucleation. The methods of quantum chemistry have increasingly been employed to model nucleation due to their high accuracy and efficiency in calculating configurational energies; and nucleation rates can be obtained from the associated free energies of particle formation. However, even in such advanced approaches, it is typically assumed that the nuclei have a classical nature, which is questionable for some systems. The importance of zero-point motion (also known as quantum nuclear dynamics) in modelling small clusters of sulphuric acid and water is tested here using the path integral molecular dynamics method at the density functional level of theory. The general effect of zero-point motion is to distort the mean structure slightly, and to promote the extent of proton transfer with respect to classical behaviour. In a particular configuration of one sulphuric acid molecule with three waters, the range of positions explored by a proton between a sulphuric acid and a water molecule at 300 K (a broad range in contrast to the confinement suggested by geometry optimisation at 0 K) is clearly affected by the inclusion of zero point motion, and similar effects are observed for other configurations.
[http://dx.doi.org/10.1063/1.4860973]

I. INTRODUCTION

The role of sulphuric acid in the formation of cloud condensation nuclei (CCN) is believed to be significant,[1,2] on account of its low vapour pressure, relatively high atmospheric concentration, and its affinity to water. However, simple attempts to understand the binary nucleation of sulphuric acid and water in detail have proved problematic. It is clear that classical nucleation theory (CNT) is insufficient for describing this process, since the critical cluster size suggested from experimental data appears to be small, and consequently several extensions and alternatives have been studied.[3–5]

One approach, the use of atomistic models that explicitly treat individual molecules or atoms within numerical simulations, has proliferated as a consequence of increasing computational power; especially based on quantum chemistry methods which treat the electronic interactions explicitly. Popular quantum chemistry methods include electronic density functional theory (DFT)[6–16] and Møller-Plesset perturbation theory (MPn where n refers to the order of the perturbation).[10,14,16,17] The usual strategy is to identify the lowest energy molecular configuration and then to use the rigid-rotor-harmonic-approximation (RRHO) to compute free energies, and thereby investigate cluster stability and nucleation through specific growth and decay routes.

The Born-Oppenheimer approximation[18] is employed by both DFT and MPn. It involves the separation of the wavefunctions of electrons and nuclei followed by a classical treatment of the dynamics of the nuclei. The DFT approach has been used to describe sulphuric acid and water clusters.[19–21] In simulations based on such approaches, the sulphuric acid and water system has been observed to exhibit proton transfers. Such events are of particular importance in this system and a challenge to the modelling. A question that arises is whether we can account for such processes correctly while representing the nuclei as classical particles. Might a quantum treatment of the proton dynamics be more accurate? Perhaps the additional uncertainty in proton position can alter the delicate balance between neutral and ionised structures? In this paper we employ Path Integral Molecular Dynamics (PIMD) to study the quantum nuclear degrees of freedom (also known as zero-point motion) of sulphuric acid/water molecular clusters to address this question. A particular issue for consideration is the level of hydration of a single sulphuric acid molecule that is required for proton transfer to occur, a matter that can be addressed either by zero temperature calculations or dynamics performed at finite temperature. It has been suggested that the threshold is around three or more water molecules.[13] Transfer of the second proton was studied by Ding and Laasonen[14] who concluded that it is likely for a level of hydration of around eight or nine water molecules.

PIMD emulates the quantum behaviour of a particle by using a classical quasiparticle or bead description, a detailed derivation of which is given by Tuckerman.[22] The PIMD method has been shown to have a significant effect on the properties in some hydrogen bonded systems.[23,24] PIMD has been employed previously together with a parametrised version of the PM6 model[25] (a semi-empirical model of

a)Electronic mail: j.stinson@ucl.ac.uk

electronic structure) to study sulphuric acid and water clusters.[26,27] Kakizaki *et al.*[26] concluded that the PIMD technique (using the normal mode transformation[22]) increased thermal fluctuations and produced more liquid-like behaviour in systems at a temperature of 250 K.[26] Sugawara *et al.*[27] studied the degree of hydration required for the first and second ionisation events for the sulphuric acid molecule, and concluded that the first ionisation takes place when four water molecules are present in the cluster in agreement with earlier work.[13] The second ionisation event occurred in the presence of 10–12 water molecules in contrast with the study by Ding and Laasonen,[14] though the latter was based on geometry optimisation techniques rather than on molecular dynamics. As the purpose of this paper was to gauge the importance of zero-point motion in the sulphuric acid and water system as accurately as possible, it was decided to use DFT rather than the semi-empirical PM6 model developed by Kakizaki *et al.*[26]

We study the importance of zero-point motion in a small cluster of sulphuric acid and water using PIMD[22,28] as implemented in the CASTEP code.[29] Section II describes the theory used, Sec. III details our results, and Sec. IV concludes our study where we comment on the significance of zero-point motion in the sulphuric acid and water system.

II. METHODS

According to the PIMD technique each particle (nucleus) is represented by a set of quasiparticles (known as beads) connected by harmonic springs. The following Hamiltonian describing the bead dynamics can be derived using the Trotter approximation,[22]

$$\mathcal{H}(x_k, p_k) = \sum_{k=1}^{P} \left[\frac{p_k^2}{2m'} + \frac{1}{2} m\omega_P^2 (x_{k+1} - x_k)^2 + \frac{1}{P} U(x_k) \right],$$

under the condition $x_{P+1} = x_1$, where P is the number of beads and x_k and p_k are, respectively, the position and momentum of bead k. ω_P is the harmonic frequency of the inter-bead springs and is given by $\sqrt{P}/\beta\hbar$ where $\beta = (k_B T)^{-1}$ and T and k_B are the system temperature and the Boltzmann constant, respectively. While m denotes the mass of the particle, the mass of the beads is represented by m', and $U(x_k)$ is the classical potential in which the particle moves. The quantum nuclear behaviour is reflected in both the position and momentum of the beads under the influence of this Hamiltonian, which is controlled by the stiffness of the inter-bead springs. Since the latter is proportional to the mass of the particle, the hydrogen nucleus is expected to be the most susceptible to zero-point effects.

Figure 1 is a snapshot from a 16 bead simulation representing the behaviour of a cluster of one sulphuric acid and four water molecules. The spatial separation of the beads clearly illustrates the greater positional uncertainty of the hydrogen nuclei compared to that of the oxygen and the sulphur nuclei.

Molecular dynamics simulations at 300 K incorporating both classical nuclear dynamics and PIMD were performed using the CASTEP[29] (version 5.5) code. The standard on-the-fly ultrasoft pseudopotential provided internally

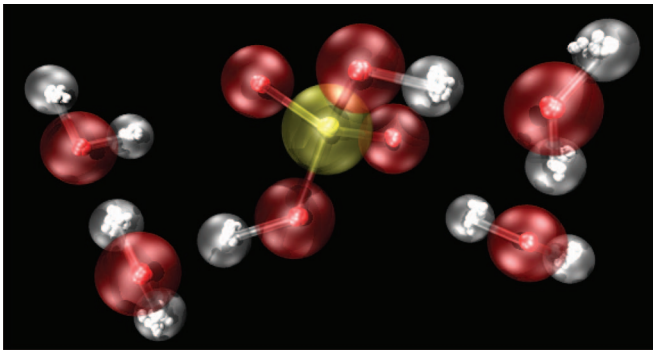

FIG. 1. A 16 bead representation of a system containing one sulphuric acid and four water molecules: the distribution of bead positions conveys the quantum uncertainty.

by the CASTEP code was employed for all calculations. The Perdew-Burke-Ernzerhof[30] (PBE) functional was used with a plane wave basis set. The PBE functional has been found to perform well for hydrogen bonded systems.[31,32] A cut off energy of 550 eV was found to converge the plane wave basis set sufficiently for all systems studied. A time step of 1 fs was used for classical (single bead) simulations and a time step of 0.5 fs or shorter was used for the PIMD simulations due to the stiffness of the inter-bead springs. CASTEP utilizes the Born-Oppenheimer version of *ab initio* MD and the Langevin thermostat with a friction constant of 0.01 fs^{-1} was used in all simulations. The equilibration period was judged by observing when the running mean energy of the system had relaxed (usually requiring less than 0.5 ps) and also by monitoring the distribution of cluster "temperature" (or kinetic energy in the centre of mass frame), which ought to be approximately Gaussian[33] with a standard deviation (σ) obeying $\sigma/\langle T \rangle \sim N^{-1/2}$. A typical temperature histogram satisfying this requirement is shown in Figure 3. The inset in Figure 3 shows that the typical relaxation time was in the order of 0.5 ps. Initial configurations of sulphuric acid and water identified from the literature were constructed under a classical potential (MMFF94s) using the Avogadro[34] (version 1.0.3) package. The choices of time step and simulation time for various cases are given in Table I.

TABLE I. Compilation of the simulation length and time step for the MD runs performed. SATH refers to sulphuric acid trihydrate and SAQH refers to sulphuric acid tetrahydrate, structures that assume typical configurations shown in Figures 2(a) and 2(b), respectively. Config H refers to the trihydrate configuration shown in Figure 4(a). Note that the longest simulations were performed for SATH and config H.

	Time step (fs)	Simulation time (ps)
SATH 1 bead	1.00	11.000
SATH 4 bead	0.50	1.500
SATH 8 bead	0.25	0.875
SATH 16 bead	0.50	10.673
SATH 32 bead	0.50	0.512
SAQH 1 bead	1.00	1.000
SAQH 4 bead	0.50	1.500
SAQH 8 bead	0.50	1.500
SAQH 16 bead	0.50	1.500
config H 1 bead	1.00	10.900
config H 16 bead	1.00	10.647

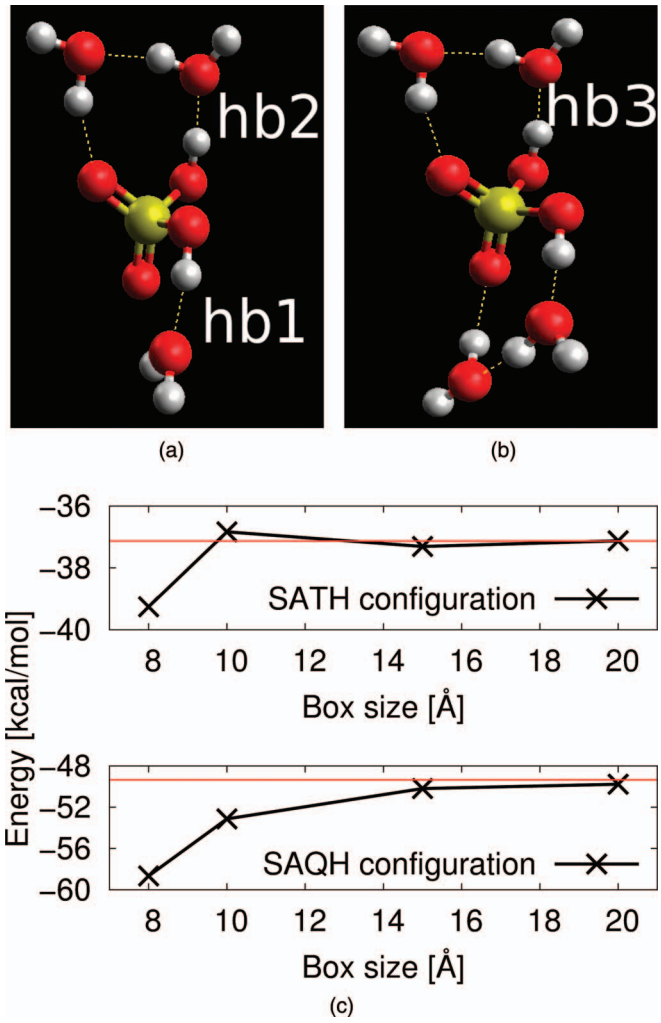

FIG. 2. Geometry optimised configurations for tri- and tetrahydrated (SATH and SAQH) clusters are shown in (a) and (b), respectively. The labelling of various hydrogen bonds is referred to in Sec. III B. Panel (c) shows the binding energies of configurations (a) and (b) as a function of the system box size, converging to values obtained by Temelso *et al.*[17] at the MP2 level.

Configurations of $[H_2SO_4][H_2O]_{n=3-4}$ were studied at a target temperature of 300 K. PIMD uses a certain number of beads to approximate the zero-point motion, and cases with $P = 1$, 4, 8, 16, and 32 beads were tested in this study. The staging transformation[22] was used for all PIMD simulations. The $P = 1$ case represents the classical limit of the PIMD technique and corresponds to the complete neglect of zero-point motion. The box size of the system was optimised against MP2 level data[17] as shown in Figure 2(c). The binding energies, at zero temperature, of the two configurations in Figures 2(a) and 2(b) are compared against MP2 level data. A box size of 15 Å was chosen as a compromise between accuracy and computational demand.

III. RESULTS

A. DFT without zero-point motion

Molecular configurations likely to feature a dissociated sulphuric acid molecule were identified from the literature

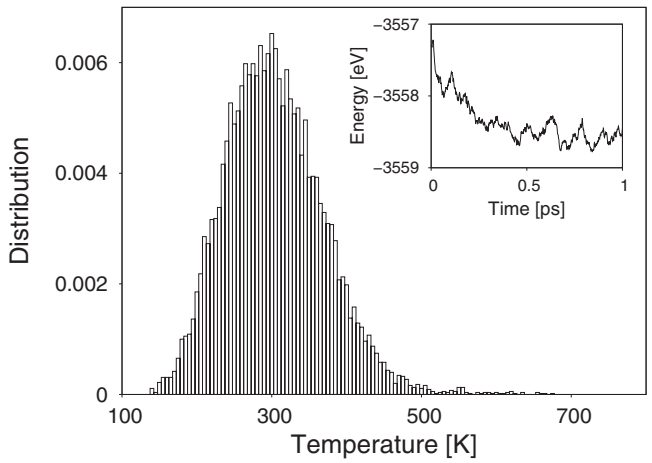

FIG. 3. Histogram of cluster kinetic energy (represented as a temperature) from the equilibrated simulation referred to as SATH 1 bead in Table I. The inset shows the system's energy as a function of time for the first 1 ps of the same simulation.

and investigated. One such configuration was labelled III-i-1 by Re *et al.*[6] and is illustrated here in Figure 4(a) and denoted config H. Our single bead simulations at 300 K show that the proton labelled H1 moves with considerable freedom between oxygens O1 and O5. Furthermore, Figure 4(b) demonstrates an anticorrelation between the length R_c of the dissociating bond O1–H1 and the sum of the lengths of the neighbouring hydrogen bonds, labelled O3–H7 and O4–H6 in Figure 4(a), and denoted R_{hy}. The formation of the "ionised" state due to the switch to the O5–H1 bond (such that the value of R_c is large) is seen to depend upon the prior existence of both the neighbouring hydrogen bonds (namely, a low value of R_{hy}). If either neighbouring hydrogen bond is broken the system remains "neutral" (with a low value of R_c), which is not surprising, since the configuration is then similar to the SATH structure shown in Figure 2. This is an important corollary to conclusions acquired from consideration of geometry optimisation at 0 K, where config H has been shown to ionise.[6] At 300 K the behaviour can most certainly not be represented by harmonic fluctuations about an ionised mean structure and a free energy based on the rigid-rotor-harmonic-approximation for this configuration would fail due to significant anharmonic contributions. We shall return to this system in Sec. III B.

B. PIMD

A PIMD study was performed first for two low energy configurations (denoted SATH and SAQH) identified in the literature[6,7] and shown in Figures 2(a) and 2(b). It is envisaged that hydrogen bonds, in particular those associated with the sulphuric acid, would be the most susceptible to zero-point effects due to the inherent tendency of sulphuric acid to dissociate. Figure 5 shows the average oxygen-oxygen distance (d_{OO}) of specific hydrogen bonds as a function of the number of beads representing atoms in the system. The bonds labelled hb1 and hb2 in the SATH structure contract in length by around 2%–5% with respect to the outcome of classical

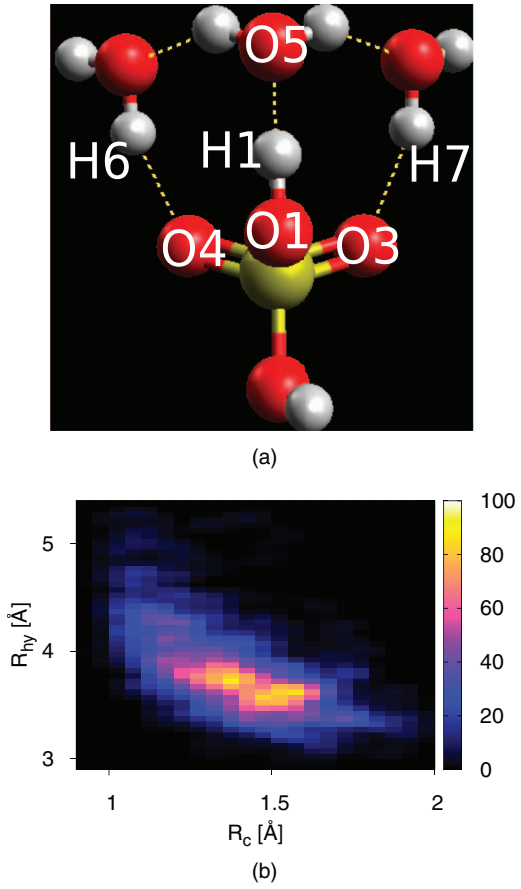

FIG. 4. The configuration denoted config H is shown in (a) with labels that identify certain O–H pairs. Plot (b) illustrates the probability density (given in arbitrary units) as a function of two structural features labelled R_c (the length of the covalent bond O1–H1) and R_{hy} (the sum of the lengths of prospective hydrogen bonds O4–H6 and O3–H7), obtained at DFT level, equivalent to using a single bead in PIMD. The associated potential of mean force takes the form of a broad, shallow well where the ionisation of the configuration is correlated with the status of the adjacent hydrogen bonds, as denoted by R_{hy}.

dynamics while the situation for hb3 is less clear. Note that the longest simulations were performed for the single bead and 16 bead representations of the SATH structure, as indicated in Table I. For other cases shorter studies were performed to illustrate the trends, though the accuracy of the results is lower.

Next we examine in detail how the behaviour of the hydrogen atom in hydrogen bond hb2 is affected by PIMD. This is explored by constructing a potential of mean force (PMF) for the hydrogen, defined by

$$W(R, \beta) = -k_B T \ln g(R, \beta),$$

where R and β are geometric parameters illustrated in Figure 6(a) and $g(R, \beta)$ is the proportion of simulation snapshots with the hydrogen located within the region defined by $R \rightarrow R + dR$ and $\beta \rightarrow \beta + d\beta$ divided by the equivalent proportion for noninteracting particles. For the PIMD simulations the centroid of the beads representing the hydrogen atom was used to produce the PMF. The method is described extensively by Kumar *et al.*[37] Figures 6(b) and 6(c) show the PMFs acquired using classical MD and PIMD, respectively, for hydrogen bond hb2.

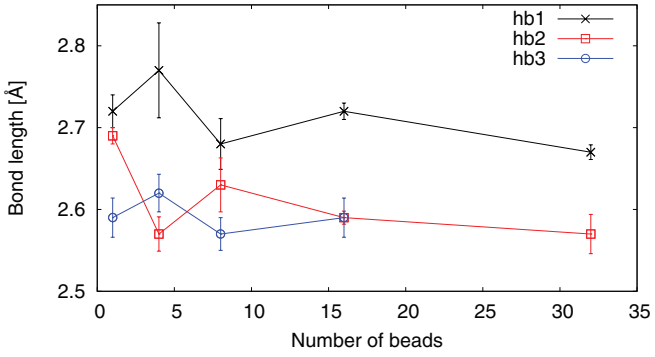

FIG. 5. The average oxygen-oxygen separation d_{OO} of specific hydrogen bonds as a function of the number of beads used in the simulation. Labels hb1 and hb2 refer to Figure 2(a) and hb3 is shown in Figure 2(b). The error bars were determined by the standard blocking procedure[35,36] and a blocking length of 0.256 ps was found to give independent sampling. The calculations correspond to the cases listed in Table I.

The PMF plots in Figure 6 visualise the differences between the dynamics of the hb2 bond in Figure 2(a) under classical MD and the PIMD schemes. Such a comparison is limited by the computationally expensive techniques employed. However, it does offer an insight into the importance of zero-point effects in small clusters of sulphuric acid and water. The main effect is a shift in the minimum of the PMF of hydrogen bond length R by about 0.2 Å going from the DFT to the PIMD result indicating that the zero-point motion has a mean configurational influence on this bond. Figure 6(d) is a one-dimensional version of Figures 6(b) and 6(c) obtained by integrating over the β parameter.

The effects of zero-point motion are clearly rather subtle. To explore this further, we return to the delicate switching behaviour of the O1–H1–O5 bonds discussed in Sec. III A and contrast the classical and quantum nuclear dynamics. Figure 7 illustrates the motion of the proton between the neutral and ionised positions, discussed earlier, in terms of the O1–H1 bond length. Which of the nuclei O1 or O5 was the nearest neighbour to the H1 nucleus (see Figure 4(a)) was monitored to quantify this hopping behaviour. It was found that in the classical case H1 was closer to O1 for 21.5% percent of the simulation with standard error $\sigma_{SE} = 3.2\%$, whereas in the 16 bead PIMD simulation this figure dropped to 14.8% with $\sigma_{SE} = 2.7\%$. This property was further investigated by defining a threshold for the O1–H1 bond length below which the system is considered neutral, and beyond which it is better described as ionised. We define a 1.22 Å; distance to separate the two regimes, and this is shown as a horizontal line in Figure 7. For the classical dynamics, the percentage of time the system remains neutral according to this criterion is 20.1% with $\sigma_{SE} = 2.9\%$. An analysis of the PIMD simulation with 16 beads yields a corresponding percentage of neutral residence time of 12.5% with $\sigma_{SE} = 2.4\%$. These results are consistent with those determined from the nearest neighbour criterion. The proportion of time spent in the ionised configuration rises from 79.1% to 87.5%. This suggests that the inclusion of zero-point motion promotes the formation of the ionised state; quantum uncertainty favours proton transfer.

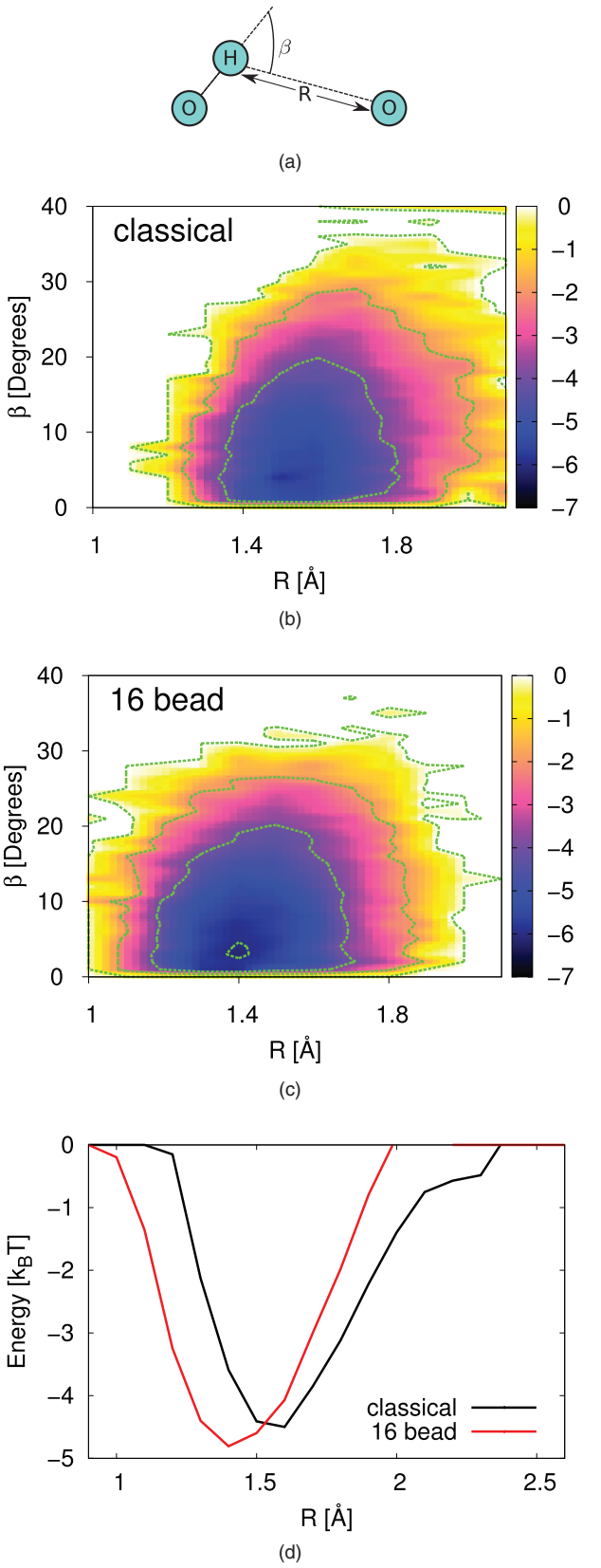

FIG. 6. Contour plots of the potential of mean force $W(R, \beta)$ in units of $k_B T$ for the hydrogen in the bond labelled hb2 in Figure 2(a). The green dashed lines indicate contour levels of 0, −2, −4, and −6. The coordinates for the PMF are defined by sketch (a) and the method follows the approach described by Kumar *et al.*[37] Plot (b) shows results from standard DFT molecular dynamics and plot (c) arises from PIMD using 16 beads. The simulation times are given in Table I. Plot (d) shows a 1D version of plots (b) and (c) obtained by integrating over the β parameter.

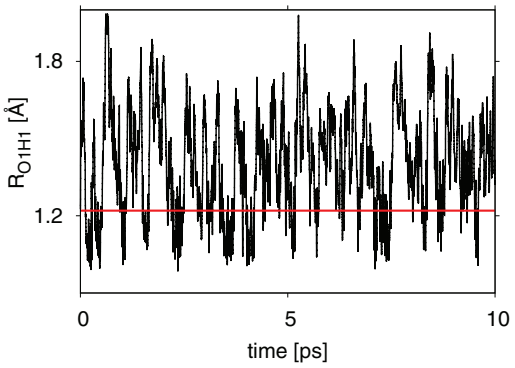

FIG. 7. Plot of the O1–H1 bond length (denoted as R_{O1H1}) against time in config H in Figure 4(a) from the 1 bead simulation as detailed in Table I. The plot clearly illustrates the motion between the neutral and ionised states. The horizontal line drawn at 1.22 Å provides a simple threshold between covalent and hydrogen bond-like behaviour of the O1–H1 bond. Under quantum nuclear dynamics the fraction of time spent above this threshold increases in the order of 10%.

IV. CONCLUSIONS

As a consequence of the computational expense of the PIMD technique, especially when using many beads, the simulations presented are limited in duration to around 10 ps for some configurations, and rather less for others. The statistics on the structural and dynamical behaviour are therefore preliminary. However, it is possible to extract some important features from these simulations that correspond to intuitive expectation, and which can be explored further with more extensive calculations.

Our study of small clusters of water and sulphuric acid molecules leads us to two main conclusions. First, we have demonstrated that molecular dynamics can reveal features that are not available from knowledge of the geometry optimised structure at zero temperature. The prime example of this is the complex behaviour of cluster configuration III-i-1 identified by Re *et al.*[6] and here denoted config H. This configuration has been regarded as the most stable ionised configuration for the trihydrated sulphuric acid molecule,[6,7,17] but our results indicate that the structure exhibits both neutral and ionised characteristics at 300 K. This conclusion highlights the limitations of the RRHO approximation[38,39] for free energy estimation using a single optimised structure.

Second, the inclusion of zero-point motion through PIMD simulations of the sulphuric acid-water system has been shown to produce small but clear structural distortion at 300 K in a selected number of configurations when compared with classical dynamics. The mean oxygen-oxygen separation of hydrogen bonds hb1 and hb2 in the structure shown in Figure 2(a) is reduced by 2%–5%. We observe a mild shortening of the hb2 hydrogen bond length, shown by constructing potentials of mean force for the classical and PIMD schemes, as illustrated in Figure 6. Furthermore, our results indicate that zero-point motion brings about a greater propensity for proton transfer in the O1–H1–O5 substructure of the configuration shown in Figure 4(a) at 300 K.

This conclusion is consistent with the paper by Li *et al.*[23] where quantum nuclear effects on the hydrogen bond are studied, specifically Figure 3 in Ref.23 where the OO length is

compared with the length of the projection of the covalent OH bond on the OO vector. The implication is that the projected covalent bond length is increased by quantum effects when the hydrogen bond is considered to be strong, as judged by a shift in vibrational frequency of the covalent OH bond due to the presence of the hydrogen bond.

Our research supports the view that the zero-point effect is most significant in configurations where proton transfer is intrinsically likely. Classical and PIMD simulations of the cluster shown in Figure 4(a) have demonstrated frequent proton transfer. Using an O–H separation of 1.22 Å as a threshold for distinguishing the ionised from the neutral state, the cluster is found to remain neutral 20.1% of the time ($\sigma_{\mathrm{SE}} = 2.9\%$) with classical MD and 12.5% ($\sigma_{SE} = 2.4\%$) according to PIMD. It is possible to infer that quantum effects have increased the degree of proton transfer. It is expected that simulations at lower temperatures would increase the significance of the zero-point effects, making this an avenue for future research. In addition, since substances such as ammonia and amines are increasingly thought to be relevant to atmospheric nucleation,[40,41] assessing the importance of zero-point motion in these systems would also be of interest.

In summary, zero-point motion does affect the structure of small clusters of sulphuric acid and water, particularly the lengths of hydrogen bonds. At 300 K, the contribution appears to be most significant for cases that are intrinsically susceptible to proton transfer.

ACKNOWLEDGMENTS

We thank Professor Angelos Michaelides and his group at UCL for practical advice and helpful discussions; and this work benefited from interactions within the Thomas Young Centre. S.M.K. was supported by the U.S. Department of Energy, Office of Basic Energy Sciences, Division of Chemical Sciences, Geosciences, and Biosciences. J.L.S. was supported by the IMPACT scheme at UCL and by the U.S. Department of Energy, Office of Basic Energy Sciences, Division of Chemical Sciences, Geosciences, and Biosciences. We are grateful for use of the UCL Legion High Performance Computing Facility and the resources of the National Energy Research Scientific Computing Center (NERSC), which is supported by the U.S. Department of Energy, Office of Science under Contract No. DE-AC02-05CH11231.

[1] *Geoengineering the Climate: Science, Governance and Uncertainty* (The Royal Society, 2009).
[2] R. Zhang, A. Khalizov, L. Wang, M. Hu, and W. Xu, Chem. Rev. **112**, 1957 (2012).
[3] I. J. Ford, Proc. Inst. Mech. Eng., Part C: J. Mech. Eng. Sci. **218**, 883 (2004).
[4] H. Vehkamäki, *Classical Nucleation Theory in Multicomponent Systems* (Springer, 2006).
[5] I. Napari, J. Julin, and H. Vehkamäki, J. Chem. Phys. **133**, 154503 (2010).
[6] S. Re, Y. Osamura, and K. Morokuma, J. Phys. Chem. A **103**, 3535 (1999).
[7] A. R. Bandy and J. C. Ianni, J. Phys. Chem. A **102**, 6533 (1998).
[8] J. C. Ianni and A. R. Bandy, J. Mol. Struct.: THEOCHEM **497**, 19 (1999).
[9] H. Arstila, K. Laasonen, and A. Laaksonen, J. Chem. Phys. **108**, 1031 (1998).
[10] L. J. Larson, M. Kuno, and F.-M. Tao, J. Chem. Phys. **112**, 8830 (2000).
[11] C.-G. Ding, K. Laasonen, and A. Laaksonen, J. Phys. Chem. A **107**, 8648 (2003).
[12] A. A. Natsheh, A. B. Nadykto, K. V. Mikkelsen, F. Yu, and J. Ruuskanen, J. Phys. Chem. A **108**, 8914 (2004).
[13] C. Arrouvel, V. Viossat, and C. Minot, J. Mol. Struct.: THEOCHEM **718**, 71 (2005).
[14] C.-G. Ding and K. Laasonen, Chem. Phys. Lett. **390**, 307 (2004).
[15] A. B. Nadykto, F. Yu, and J. Herb, Phys. Chem. Chem. Phys. **10**, 7073 (2008).
[16] T. Kurtén, I. K. Ortega, and H. Vehkamäki, J. Mol. Struct.: THEOCHEM **901**, 169 (2009).
[17] B. Temelso, T. E. Morrell, R. M. Shields, M. A. Allodi, E. K. Wood, K. N. Kirschner, T. C. Castonguay, K. A. Archer, and G. C. Shields, J. Phys. Chem. A **116**, 2209 (2012).
[18] R. M. Martin, *Electronic Structure: Basic Theory and Practical Methods* (Cambridge University Press, 2004).
[19] Y.-K. Choe, E. Tsuchida, and T. Ikeshoji, J. Chem. Phys. **126**, 154510 (2007).
[20] K. E. Anderson, J. I. Siepmann, P. H. McMurry, and J. VandeVondele, J. Am. Chem. Soc. **130**, 14144 (2008).
[21] A. Hammerich, V. Buch, and F. Mohamed, Chem. Phys. Lett. **460**, 423 (2008).
[22] M. E. Tuckerman, *Statistical Mechanics: Theory and Molecular Simulations* (Oxford University Press, 2010).
[23] X.-Z. Li, B. Walker, and A. Michaelides, Proc. Natl. Acad. Sci. **108**, 6369 (2011).
[24] B. Walker and A. Michaelides, J. Chem. Phys. **133**, 174306 (2010).
[25] J. J. P. Stewart, J. Mol. Model. **13**, 1173 (2007).
[26] A. Kakizaki, H. Motegi, T. Yoshikawa, T. Takayanagi, M. Shiga, and M. Tachikawa, J. Mol. Struct.: THEOCHEM **901**, 1 (2009).
[27] S. Sugawara, T. Yoshikawa, T. Takayanagi, M. Shiga, and M. Tachikawa, J. Phys. Chem. A **115**, 11486 (2011).
[28] R. P. Feynman and A. R. Hibbs, *Quantum Mechanics and Path Integrals: Emended Edition (Dover Books on Physics)* (Dover Publications, 2010).
[29] S. J. Clark, M. D. Segall, and C. J. Pickard, Z. Kristallogr. **220**, 567 (2005).
[30] J. Perdew, K. Burke, and M. Ernzerhof, Phys. Rev. Lett. **77**, 3865 (1996).
[31] K. S. Thanthiriwatte, E. G. Hohenstein, L. A. Burns, and C. D. Sherrill, J. Chem. Theory Comput. **7**, 88 (2011).
[32] J. Ireta, J. Neugebauer, and M. Scheffler, J. Chem. Phys. A **108**, 5692 (2004).
[33] J. M. Haile, *Molecular Dynamics Simulation: Elementary Methods (Wiley Professional)* (Wiley-Interscience, 1997), p. 512.
[34] M. D. Hanwell, D. E. Curtis, D. C. Lonie, T. Vandermeersch, E. Zurek, and G. R. Hutchison, J. Cheminf. **4**, 17 (2012).
[35] H. Flyvbjerg and H. G. Petersen, J. Chem. Phys. **91**, 461 (1989).
[36] D. Frenkel and B. Smit, *Understanding Molecular Simulations: From Algorithms to Application*, 2nd ed. (Elsevier, 2001).
[37] R. Kumar, J. R. Schmidt, and J. L. Skinner, J. Chem. Phys. **126**, 204107 (2007).
[38] S. Kathmann, G. Schenter, and B. Garrett, Phys. Rev. Lett. **98**, 109603 (2007).
[39] S. Kathmann, G. Schenter, and B. Garrett, J. Phys. Chem. C **111**, 4977 (2007).
[40] T. Kurtén, V. Loukonen, H. Vehkamäki, and M. Kulmala, Atmos. Chem. Phys. Discuss. **8**, 7455 (2008).
[41] J. Kirkby, J. Curtius, J. Almeida, E. Dunne, J. Duplissy, S. Ehrhart, A. Franchin, S. Gagné, L. Ickes, A. Kürten, A. Kupc, A. Metzger, F. Riccobono, L. Rondo, S. Schobesberger, G. Tsagkogeorgas, D. Wimmer, A. Amorim, F. Bianchi, M. Breitenlechner, A. David, J. Dommen, A. Downard, M. Ehn, R. C. Flagan, S. Haider, A. Hansel, D. Hauser, W. Jud, H. Junninen, F. Kreissl, A. Kvashin, A. Laaksonen, K. Lehtipalo, J. Lima, E. R. Lovejoy, V. Makhmutov, S. Mathot, J. Mikkilä, P. Minginette, S. Mogo, T. Nieminen, A. Onnela, P. Pereira, T. Petäjä, R. Schnitzhofer, J. H. Seinfeld, M. Sipilä, Y. Stozhkov, F. Stratmann, A. Tomé, J. Vanhanen, Y. Viisanen, A. Vrtala, P. E. Wagner, H. Walther, E. Weingartner, H. Wex, P. M. Winkler, K. S. Carslaw, D. R. Worsnop, U. Baltensperger, and M. Kulmala, Nature (London) **476**, 429 (2011).